Blind Color Image Fusion Based on the Optimal Multi-objective Particle Swarm Optimization

Lincheng Shen and Yifeng Niu

College of Mechatronic Engineering and Automation
National University of Defense Technology
{lcshen, niuyifeng}@nudt.edu.cn

Abstract

The particle swarm optimization (PSO) is a new swarm intelligence technique inspired by social behavior of bird flocking. In this paper, the optimal multi-objective particle swarm optimization (OMOPSO) is presented. Since the parameters determine the optimization performance of the algorithm, the uniform design is introduced to obtain the optimal combination of the parameters. Additionally, a new crowding operator is used to improve the distribution of nondominated solutions, and ε-dominance is used to fix the size of the set of final solutions. OMOPSO is applied to optimize the parameters of blind color image fusion. First the model of blind color image fusion in YUV color space is established, and then the proper evaluation metrics without the reference image are given, in which a new metrics of conditional mutual information is proposed. Experimental results indicate that the method of blind color image fusion based on OMOPSO realizes the Pareto optimal blind color image fusion.

Keyword*: Blind color image fusion, Particle swarm optimization, Multi-objective optimization, Uniform design*

1. Introduction

At present, multi-objective evolutionary algorithms include Pareto Archive Evolutionary Strategy (PASE) [1], Strength Pareto Evolutionary Algorithm (SPEA2) [2], Nondominated Sorting Genetic Algorithm II (NSGA-II) [3], Multiple Objective Particle Swarm Optimization (MOPSO) [4], etc, where MOPSO has a higher convergence speed and better optimization capacities [5]. However, MOPSO uses an adaptive grid [1] to record the searched particles, once the number of the objectives is greater than 3, MOPSO will need too much computing time. So we presented an adaptive multi-objective particle swarm optimization (AMOPSO) in [6], in which the adaptive grid is discarded, and a crowding distance [3], an adaptive inertia weight and an adaptive mutation are introduced to improve the search capacity. But the crowding distance needs too much time and the optimal combination of the parameters is difficult to obtain, so we propose OMOPSO (the Optimal MOPSO). OMOPSO introduces the uniform design to obtain the optimal combination of parameters, adopts a new crowding distance based on sorting to decrease the complexity, and uses the ε-dominance to keep the size of the external archive. In contrast to MOPSO and AMOPSO, OMOPSO has a higher convergence speed and better exploratory capabilities.

Blind color image fusion can be defined as the process of combining two or more color images into a single composite image with extended information content [7], in the case that the reference image doesn't exist. In fact, color image fusion can be regarded as an optimization problem using several source images, and there are various kinds of evaluation

metrics. In order to realize the optimal image fusion, it is highly necessary to introduce multi-objective optimization algorithms to search the optimal parameters. In [6], an approach to image fusion in the gray-scale space based on multi-objective optimization was explored. However, for the blind color image fusion, a nave approach might include performing image fusion separately and independently on each color channel, then providing the resulting three color channels as a single color image. In practice, this does not work for two reasons: interpretation of color scale space for feature selection and dependencies between the color components. Furthermore, the reference image may not exist in many cases. Therefore, the approach to blind color image fusion in YUV color space is presented, and OMOPSO is used to optimize the fusion parameters.

The remainder of this paper is organized as follows. The OMOPSO algorithm is designed in Sect. 2. The methodology of blind color image fusion is introduced in Sect. 3. The evaluation metrics are given in section Sect. 4. The experimental results and analysis are given in Sect. 5. Finally, a review of the results and the future research areas are discussed in Sect. 6.

2. OMOPSO Algorithm

Kennedy and Eberhart brought forward particle swarm optimization (PSO) inspired by the choreography of a bird flock in 1995 [8]. PSO has shown a high convergence speed in multi-objective optimization [4], [5], [6]. In order to improve the performance of the algorithm, we propose "OMOPSO" (the Optimal Multi-Objective Particle Swarm Optimization), in which not only the adaptive mutation operator and the adaptive inertia weight is used to raise the searching capacity, but also the uniform design is used to obtain the optimal combination of the algorithm parameters, a new crowding operator is used to improve the distribution of nondominated solutions along the Pareto front and maintain the population diversity, and the ε-dominance is used to keep the capacity of the external archive.

2.1. OMOPSO Flow

The flow of OMOPSO is the following.

Step 1. Initialize the position of each particle: $pop[i]$=arbitrary, where $i=1,...,NP$, NP is the particle number; initialize the velocity of each particle: $vel[i]=0$; initialize the record of each particle: $pbests[i]=pop[i]$; evaluate each of the particles in the POP where POP is defined as $\{pop[1], ..., pop[N_P]\}$: $fun[i, j]$, where $j=1,...,NF$, and NF is the objective number; and store the positions that represent nondominated particles in the repository of the REP according to the Pareto optimality, where REP is defined as $\{rep[1], ..., rep[N_P]\}$, then send the resolutions in the REP to the ε-archive.

Step 2. Update the velocity of each particle using the following expression

$$vel[i] = W \cdot vel[i] + c_1 \cdot rand_1 \cdot (pbests[i] - pop[i]) + c_2 \cdot rand_2 \cdot (rep[h] - pop[i]) \quad (1.)$$

where W is the adaptive inertia weight; c_1 and c_2 are the learning factors [5], $rand_1$ and $rand_2$ are random values in the range [0, 1]; $pbests[i]$ is the best position that particle i has had; h is the index of the resolution in the repository with maximum

crowding distance that implies the particle is located in the sparse region, as aims to maintain the population diversity; $pop[i]$ is the current position of particle i.

Step 3. Update the new positions of the particles adding the velocity produced from the previous step.

$$pop[i] = pop[i] + vel[i] \quad (2.)$$

Step 4. Maintain the particles within the search space in case they go beyond their boundaries (to avoid generating solutions that do not lie on valid search space).

Step 5. Adaptively mutate each of the particles in the *POP* at a probability of P_m.

Step 6. Evaluate each of the particles in the *POP*.

Step 7. Update the contents in the *REP*, and insert all the current nondominated positions into the repository, then update the ε-archive.

Step 8. Update the record of each particle. When the current position of the particle is better than the position contained in its memory, the latter is updated.

$$pbests[i] = pop[i] \quad (3.)$$

Step 9. If the maximum cycle number is reached, stop the process and output the Pareto solutions in the ε- archive; else go to Step 2.

2.2. Repository Control

The external repository of REP is used to record the nondominated particles in the primary population. At the beginning of the search, the REP is empty. The nondominated vectors found at each iteration are compared with respect to the contents of the REP. If the REP is empty, the current solution will be accepted. If this new solution is dominated by an individual within the REP, such a solution will be automatically discarded. Otherwise, if none of the elements contained in the REP dominates the solution wishing to enter, such a solution will be stored in the REP. If there are solutions in the REP that are dominated by a new element, such solutions will be removed out of the REP. Finally, if the REP has reached its maximum capacity, the new nondominated solution and the contents of the REP will be combined into a new population, according to the objectives, the individuals with lower crowding distances (located in the dense region) will not enter into the REP.

2.3. ε Dominance

We adopt the concept of ε-dominance [9] in order to fix the size of the external archive that contains the (nondominated) solutions that will be reported by the algorithm. A decision vector x_1 is said to ε-dominate a decision vector x_2 for some $\varepsilon >$ 0, iff $\forall i$ (i = 1, . . . , m)

$$f_i(x_1)/(\varepsilon+1) \geq f_i(x_2) \quad (4.)$$

and for at least one i (i = 1, . . . , m)

$$f_i(x_1)/(\varepsilon+1) > f_i(x_2) \quad (5.)$$

where m is the objective number. It is worth noting that, when using ε-dominance, the size of the final external archive depends on the ε-value, which is normally a user

defined parameter [9]. For the sake of simplicity, we consider the same value of ε for all the objective functions of a given problem.

2.4. Adaptive Inertia Weight

A large inertia weight of W facilitates global exploration (searching new areas), while a small one tends to facilitate local exploration, i.e. fine-tuning the current search area. When W is in the range [0.8, 1.2], the algorithm has a higher convergence speed. Y. Shi adopted an adaptive linear weight. In order to make the algorithm have better global exploration ability at the beginning of the search, and better local exploration ability in the end, we proposed an adaptive concave exponent weight.

$$W = \frac{1}{e-1}[W_{\min} e - W_{\max} + (W_{\max} - W_{\min}) e^{1-\frac{g}{G_{\max}}}] \tag{6.}$$

where W_{min} is the minimum of the adaptive inertia weight, W_{max} is the maximum of the weight, g is the loop counter, G_{max} is the maximum number of circles.

2.5. Crowding Distance

In order to improve the distribution of nondominated solutions along the Pareto front, we introduce a concept of crowding distance from NSGA-II [3] that indicates the population density. When comparing the Pareto optimality between two individuals, we find that the one with a higher crowding distance (locating the sparse region) is superior. In [3], the crowding distance has $O(mn \log n)$ computational complexity, and may need too much time because of sorting order. Here we propose a new crowding distance that can be calculated using the level sorting. The crowding distance of the boundary points is set to infinity so that they can be selected into the next generation. The others can be calculated with respect to their objectives. For objective j, we divide its value range into special levels according to the boundary, then sort these levels in descending order of the number of the particles, and compute the crowding distance using the following expression

$$d_{ij} = S_{ij} / N_{ij} \tag{7.}$$

where d_{ij} is the crowding distance of particle i at objective j, S_{ij} is the sequence number of the level where particle i locates, N_{ij} is the number of the particles in level S_{ij}. The crowding distance of particle i is defined as

$$Dis[i] = \sum_j d_{ij} \tag{8.}$$

The new crowding distance doesn't need to sort order for every objective and has less complexity, and it is superior to the grid [1], [4] because the latter may fail to allocate memory when there exist too many objectives.

2.6. Adaptive Mutation

PSO is known to have a very high convergence speed. However, such a convergence speed may be harmful in the context of multi-objective optimization. An adaptive mutation operator is applied not only to the particles of the swarm, but also to the range of each design variable of the problem [4]. What this does is to cover the full range of each design variable at the beginning of the search and then we narrow the range covered over time, using a nonlinear function.

$$R = (Upper - Lower) \cdot (1 - g/(p_m G_{\max}))^{1.5} \tag{9.}$$

where *Upper* is the upper of the design variable, *Lower* is the lower, *R* is the value range of the variables.

2.7. Uniform Design of Parameters

We introduce the uniform design [10] to optimize the parameters of OMOPSO. The main objective of uniform design is to sample a small set of points from a given set of points, such that the sampled points are uniformly scattered. Let there be n factors and q levels per factor. When n and q are given, the uniform design selects q combinations out of q^n possible combinations, such that these q combinations are scattered uniformly over the space of all possible combinations. The selected combinations are expressed in terms of a uniform array $U(n, q)=[U_{i,j}]_{q\times n}$, where $U_{i,j}$ is the level of the j^{th} factor in the i^{th} combination. When q is prime and $q>n$, it has been proved that is given by

$$U_{i,j} = (i\sigma^{j-1} \bmod q) + 1 \tag{10.}$$

where σ is determined by the number of factors and the number of levels [10].

3. Blind Color Image Fusion in YUV Space

The result of the fusion process applied to color images should preserve the following consistency criteria from the original images: color blending consistency and color spatial consistency, i.e. color must be preserved and boundaries between colors must be preserved [7]. For our methods, we choose the YUV color space, which has components representing luminance, saturation, and hue. In the case of fusing source images, it is desired that the structural details of the image be emphasized while the color and its saturation are preserved. The edge energy of an image can usually be discerned from the gray-scale representation of the image alone, which represents the luminance band of the YUV color space. Thus, YUV is a convenient representation for assessing edge energy. As shown in Figure 1, the approach to multi-objective color image fusion in YUV color space is as follows.

Step 1: Input the source images A and B and convert the two images from RGB color space into YUV color space respectively. The conversion from RGB to YUV is given by

$$\begin{bmatrix} Y \\ U \\ V \end{bmatrix} = \begin{bmatrix} 0.299 & 0.587 & 0.114 \\ -0.148 & -0.289 & 0.437 \\ 0.615 & -0.515 & -0.100 \end{bmatrix} \begin{bmatrix} R \\ G \\ B \end{bmatrix} \tag{11.}$$

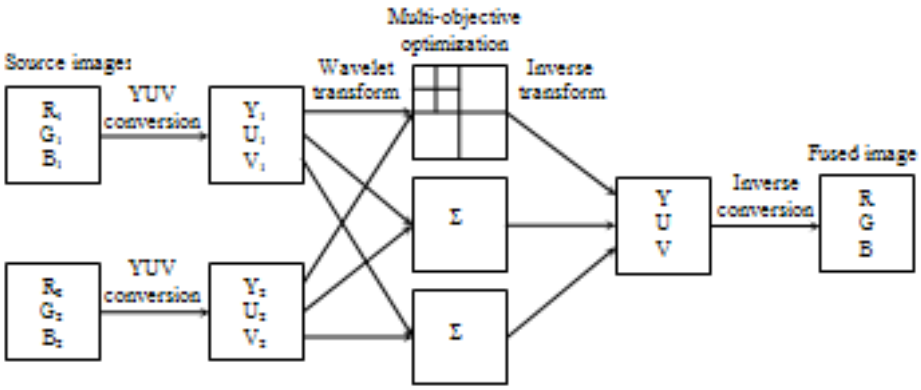

Figure 1. Illustration of multi-objective blind color image fusion in YUV space

Since the source images can be assumed to have similar saturation and hue, the average of the U and V components from source images can be substituted for the U and V components in the fused image respectively, which can also reduce the computation complexity.

Step 2: Component Y represents the luminance, hence both the selection functions are based on the discrete wavelet transform (DWT) of the luminance components. Find the DWT of component Y of A and B to a specified number of the decomposition level; we will get one approximation and $3 \times J$ details at each level, where J is the decomposition level. In general, J is not greater than 3.

Step 3: For the details of component Y in DWT domain, salient features in each source image are identified. The coefficient with the largest salience is substituted for the fused coefficient [11].

$$S_j(x,y) = \sum\sum W_j^2(x+m, y+n), \quad j = 1,\ldots,J. \tag{12.}$$

where $W_j(x, y)$ is the wavelet coefficient at location (x, y), and (m, n) defines a window of coefficients around the current coefficient. The size of the window is typically small, e.g. 3 by 3.

The coefficient with the largest salience is substituted for the fused coefficient while the less salient coefficient is discarded. The selection mode is implemented as

$$W_{Fj}(x,y) = \begin{cases} W_{Aj}(x,y) & S_{Aj}(x,y) \geq S_{Bj}(x,y) \\ W_{Bj}(x,y) & otherwise \end{cases} \tag{13.}$$

where $W_{Fj}(x, y)$ are the final fused coefficient in DWT domain, W_{Aj} and W_{Bj} are the current coefficients of A and B at level j in the Y components.

Step 4: For approximations of component Y in DWT, let C_F , C_A, and C_B be the approximations of F, A, and B respectively, two different fusion rules will be adopted. One rule called “uniform weight method (UWM)” is given by

$$C_F(x,y) = w_1 \cdot C_A(x,y) + w_2 \cdot C_B(x,y) \quad (14.)$$

where w_1 and w_2 are the decision variables with the values in the range [0, 1].

The other called "adaptive weight method (AWM)" is given by

$$C_F(x,y) = w_1(x,y) \cdot C_A(x,y) + w_2(x,y) \cdot C_B(x,y) \quad (15.)$$

where $w_1(x, y)$ and $w_2(x, y)$ are decision variables.

Step 5: Using OMOPSO, we can find the optimal decision variables of the Y component in DWT domain, and realize the optimal blind color image fusion.

Step 6: The new sets of coefficients are used to find the inverse transform to get the Y component of the fused image F.

Step 7: The fused image in RGB color space can be attained using the inverse YUV conversion.

4. Evaluation of Blind Color Image Fusion

To establish an evaluation metric system is the basis of the optimization that determines the performance of the final fused image [12]. However, in the image fusion literature only a few indices for quantitative evaluation of different image fusion methods have been proposed. Generally, the construction of the perfect fused image is an illdefined problem since in most case the optimal combination is unknown in advance. In this study, we explore the possibility to establish an impersonal evaluation metric system and get some meaningful results. In fact, the evaluation metrics of blind color image fusion can be divided into two categories with respect to the subjects reflected. One category reflects the image features, such as gradient and entropy. The second reflects the relation of the fused image to the resource images, such as conditional mutual information and information symmetry.

4.1. Gradient

Gradient reflects the change rate in the details that can be used to represent the clarity degree of an image. The higher the gradient of the fused image is, the clearer it is. In the YUV representation, Y represents the luminance of the image; hence gradient in the luminance component can also reflect the characteristics of human vision system. Gradient is given by

$$G = \frac{\sum\sum\sqrt{[Y(x,y)-Y(x+1,y)]^2 + [Y(x,y)-Y(x,y+1)]^2}}{\sqrt{2}(M-1)(N-1)} \quad (16.)$$

where M and N are the numbers of the row and column of the color image respectively.

4.2. Entropy

Entropy is an metric to evaluate the information quantity contained in an image. If the value of entropy becomes higher after fusing, it indicates that the information quantity increases and the fusion performances are improved. Entropy in one color channel is defined as

$$E_H = -\sum_{i=0}^{L} p_i \log_2 p_i \tag{17.}$$

where H=R, G, B, L is the total of gray levels of each color channel, p_i is the probability distribution of level i.

The entropy in a color image is given by

$$E = (E_R + E_G + E_B)/3 \tag{18.}$$

where R, G, and B denote the three color channel respectively, E_R denotes the entropy in channel R..

4.3. Conditional Mutual Information

Qu [13] et al adopted mutual information to represent the amount of information that is transferred from the source images to the final fused image, where no attention has been paid to the overlapping information of the source images, so this metric can't effectively evaluate the mutual information among the fused image and the source images. Tsagaris [14] proposed the conditional mutual information which can avoid overlapping information of the source images. However, the calculation expression is a little complex.

We make an improvement and get new conditional mutual information (CMI). CMI are used to evaluate the correlative performances of the fused image and the source images. Let A and B be two random variables, and joint entropy is $H(A, B)$, the conditional entropy given F is $H(A, B|F)$, the conditional mutual information is defined as

$$CMI_H = 1 - \frac{H(A,B \mid F)}{H(A,B)} \tag{19.}$$

A higher value of CMI indicates that the fused image contains fairly good quantity of information presented in both the source images. CMI takes values in the range [0, 1], where zero corresponds to total lack of common information between the source images and the fused image and one corresponds to an effective fusion process that transfers all the information from the source images to the fused image (in the ideal case). The conditional mutual information in a color image is given by

$$CMI = (CMI_R + CMI_G + CMI_B)/3 \tag{20.}$$

4.4. Information Symmetry

A high value of CMI doesn't imply that the information from both the images is symmetrically fused, e.g. when F is identical with A, CMI will be high and take the value of

$H(A)$. Therefore, we introduce the metric of information symmetry (InfS) from [15] and make an improvement. InfS is defined as

$$InfS_H = 1 - \left| \frac{I(X_2;F) - I(X_1;F)}{\max[I(X_1;F), I(X_2;F)]} \right| \quad (21.)$$

where $I(A, F)$ is the mutual information of A and F, and $I(B,F)$ is the mutual information of B and F.

InfS is an indication of how much symmetric the fused image is, with respect to input images. The higher the value of InfS is, the better the fusion result is. InfS also takes values in the range [0, 1], where zero implies that the fused image is identical with some one of source images, while one implies that both the images is symmetrically fused. The information symmetry in a color image is given by

$$InfS = (InfS_R + InfS_G + InfS_B)/3 \quad (22.)$$

5. Experiments

The performances of the proposed blind color image fusion approach using OMOPSO is tested and compared with those of different fusion schemes. The image "cemetery" from Lab. for Image and Video Engineering of Texas University is selected as the reference image of R with 256 × 256 pixels in size, each pixel being represented by three bytes (one for each of the R, G, and B channels). The two source images of A and B is shown in Figure 2(a) and Figure 2(b) We use OMOPSO to search the Pareto optimal weights of the blind color image fusion model and compare the results with those of SSM (Simple Space Method), and SWM (Simple Wavelet Method), where SSM and SWM take a fixed weight of 0.5 in spatial domain and in wavelet domain respectively. In order to get common evaluations, the sum of the weights at each position in source images is limited to 1. Since the solutions to blind color image fusion are nondominated by one another, we give preference to the four metrics so as to select the Pareto optimal solutions, e.g. one order is CMI, Gradient, InfS, Entropy.

5.1. Uniform Design of the Parameters

The more important and representative parameters of OMOPSO include the number of particles, the number of cycles, the value for bounding the size of the ε-archive, and the mutation probability. We construct a uniform array with four factors and five levels as follows, where σ is equal to 2. We compute U(4, 5) based on (10) and get

$$U(4,5) = \begin{bmatrix} 2 & 3 & 5 & 4 \\ 3 & 5 & 4 & 2 \\ 4 & 2 & 3 & 5 \\ 5 & 4 & 2 & 3 \\ 1 & 1 & 1 & 1 \end{bmatrix} \quad (23.)$$

The value range of the number of particles is [40, 120]; the range of the number of cycles is [50, 250]; the range of the value for bounding the size of the ε-archive) is [0.005, 0.009]; the range of the mutation probability is [0.02, 0.06]. All combinations are run for a maximum value of 100 evaluations. Table 1 shows the evaluation metrics of the fused images from different combinations. Results show that the third combination is the optimal in the problem. Thus, the parameters of OMOPSO are as follow: the particle number is 100; the maximum cycle number is 100; the value of ε for bounding the size of the ε-archive is 0.007; the mutation probability is 0.06.

Table 1. Evaluation of Different Combinations

Comb.	Gradient	Entropy	CMI	InfS
1	10.0314	7.4336	0.5326	0.9992
2	10.0336	7.4386	0.5346	0.9993
3	10.0423	7.4415	0.5383	0.9993
4	10.0304	7.4329	0.5362	0.9994
5	10.0293	7.4324	0.5317	0.9992

5.2. Comparison among Different Fusion Schemes

The experiments of blind color image fusion using OMOPSO are done, and the results is shown in Figure 2(e) and Figure 2(f), where the fused images at level 3 in DWT are given, for a higher level decreases the decision variables and improves the adaptability. From Figure 2, we can see that OMOPSO performs well, the results of AWM and UWM are superior to those of SWM and SSM, and the result of AWM is superior to that of UWM, because SWM and SSM cannot attain the optimal fusion parameters, and the weights of AWM are adaptive in different regions. Therefore, the approach to blind color image fusion that uses OMOPSO to search the adaptive fusion weights at level 3 in DWT domain is the optimal method. It is also be seen that this approach can overcome the limitations of given fusion parameters, obtain the optimal fusion results, and effectively enhance the features of the color image.

6. Conclusions

OMOPSO proposed is an effective algorithm to solve the parameter optimization of blind color image fusion. OMOPSO has the optimal parameter combination and is especially suitable for the case when there are too many objectives. One aspect that we would like to explore in the future is to analyze the evaluation metrics system to acquire a meaningful measurement. We are also considering improving the optimization performances of OMOPSO further.

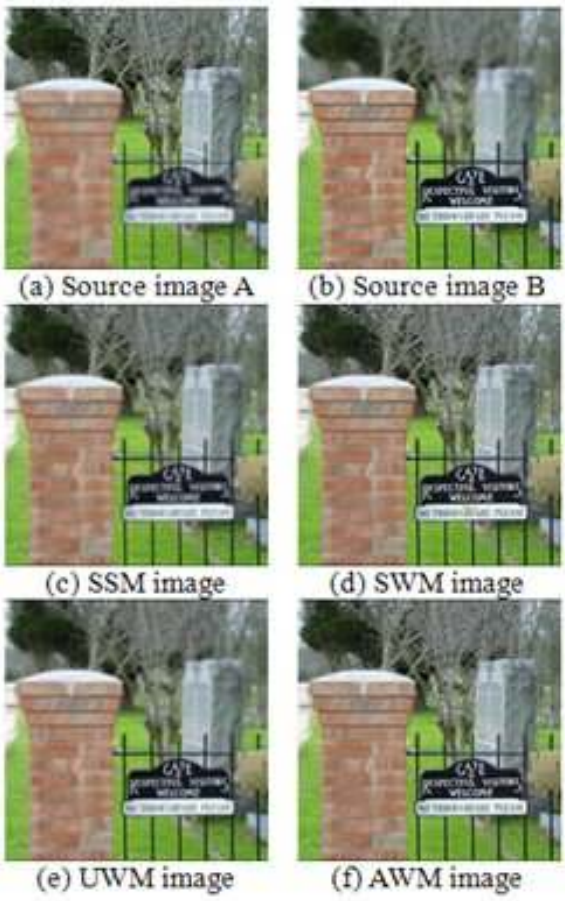

Figure 2. Source and fused images

References

[1] J.D. Knowles, D.W. Corne, "Approximating the Nondominated Front Using the Pareto Archived Evolution Strategy", Evol. Comput., Vol. 8, No. 2, pp. 149-172, Summer, 2000.
[2] E. Zitzler, M. Laumanns, L. Thiele, "SPEA2: Improving the Strength Pareto Evolutionary Algorithm", TIK-Report 103, ETH, Zurich, Switzerland, May 2001.
[3] K. Deb, A. Pratap, S. Agarwal, T. Meyarivan, "A Fast and Elitist Multiobjective Genetic Algorithm: NSGA-II", IEEE Trans. Evol. Comput., Vol. 6, No. 2, pp. 182-197, Apr. 2002.
[4] C.A. Coello, G.T. Pulido, and M.S. Lechuga, "Handling multiple Objectives with Particle Swarm Optimization", IEEE Trans. Evol. Comput., Vol. 8, No. 3, pp. 256-279, Jun. 2004.
[5] M. Reyes-Sierra, C.A. Coello Coello, "Multiobjective Particle Swarm Optimizers: a Survey of the State-of-the-art", Int. J. Comput. Intell. Research, Vol. 2, No. 3, pp. 287-308, Mar. 2006.
[6] Y.F. Niu, L.C. Shen, "A Novel Approach to Image Fusion Based on Multi-Objective Optimization", Proc. WCICA06, Dalian, Vol. 12, pp. 9911-9915, Jun. 2006.
[7] L. Bogoni, M. Hansen, "Pattern-Selective Color Image Fusion", Pattern Recogn, Vol. 34, No 8, pp. 1515-1526, Aug. 2001.

[8] J. Kennedy and R.C. Eberhart, "Particle Swarm Optimization", Proc. IEEE Int. Conf. Neural Networks, Vol. 4, pp. 1942-1948, Dec. 1995.
[9] S. Mostaghim, J. Teich, "The Role of ε-dominance in Multi Objective Particle Swarm Optimization Methods", Proc. IEEE Cong. Evolutionary Computation, Canberra, Vol. 3, pp.1764-1771, Sep. 2003.
[10] Y.W. Leung, Y.P. Wang, "Multiobjective Programming Using Uniform Design and Genetic Algorithm", IEEE Trans. Syst. Man Cybern. Pt. C: Appl. Rev., Vol.30, No 3, pp.293-304, Aug. 2000.
[11] X.S. Huang and Z Chen, "A Wavelet-Based Image Fusion Algorithm", Proc. IEEE TENCON 2002, pp. 602-605, Oct. 2002.
[12] A. Toet, M.P. Lucassen, "A Universal Color Image Quality Metric", Proc. SPIE, Vol. 5108, pp. 13-23, Apr. 2003.
[13] G.h. Qu, D.l. Zhang, P.f. Yan, "Information Measure for Performance of Image Fusion", IEE Electron. Lett., vol. 38, No. 7, pp. 313-315, Mar. 2002.
[14] V. Tsagaris, V. Anastassopoulos, "A Global Measure for Assessing Image Fusion Methods", Opt. Eng. Vol.45, No. 2, pp. 1-8, Feb. 2006.
[15] C. Ramesh and T.Ranjith, "Fusion Performance Measures and a Lifting Wavelet Transform Based Algorithm for Image Fusion", Proc. ISIF 2002, Vol.1, pp. 317-320, Jul. 2002.

Authors

Lincheng Shen

Received the B.S., M.S., and Ph.D. degree in control science and engineering from National University of Defense Technology (NUDT), Changsha, China, in 1986, 1989 and 1994. He is currently a professor of College of Mechatronic Engineering and Automation in NUDT. His current research interests include intelligent system, image processing, and information fusion.

Yifeng Niu

Received the B.S. degree in control science and engineering from National University of Defense Technology (NUDT), Changsha, China, in 2001. He is currently a Ph.D. candidate of Automation Institute in NUDT. His current research interests include image processing and information fusion.